

## Inlet Impacts on Local Coastal Processes

Rajesh Srinivas<sup>1</sup>, Associate Member, and R. Bruce Taylor<sup>1</sup>, Fellow

### Abstract

*St. Augustine Inlet, a trained, ebb-dominated inlet, acts as an efficient sediment trap by impounding sediments in ebb and, to a lesser extent, flood shoals. The ebb shoal, containing 23 million cy of sand by 1994, impounds 425,000 cy/yr of sand without signs of abatement. Inlet sand trapping causes chronic erosion of the south beach. The large inlet sand trapping capacity appears to be related to the large magnitudes of and the large mismatch between the ebb and flood discharge prisms. Spreading characteristics of the ebb jet are consistent with observed sedimentation patterns of the ebb shoal.*

### Introduction

St. Augustine Inlet, located in northeast Florida (a state in the Southeastern United States), connects the Tolomato River, flowing from the north, and the Matanzas River, flowing from the south, to the Atlantic Ocean (Figure 1). Vilano Beach and Conch Island lie to the north and south of the inlet, respectively. Salt Run, a 2.1-mile long embayment extending south from the inlet, is a relic of the old, pre-stabilization inlet.

The natural orientation of the inlet was northwest to southeast until about 1940. The U.S. Army Corps of Engineers (COE) cut a new, east-west oriented channel approximately 1,200 ft north of the natural inlet and constructed a 1,580-ft north jetty between 1940—1941. A 3,695-ft south jetty was later constructed by the COE in 1957.

This paper quantifies the inlet sand trapping effects by examining bathymetric and beach profile data, historical mechanical bypassing rates, and littoral drift in the inlet vicinity. An inlet hydrodynamic model and an ebb jet model are employed to relate the inlet sand trapping effects to inlet hydraulics.

### Bathymetric and Beach Profile Data

A COE 1937 survey of St. Augustine Inlet, supplemented by aerial photographs and an old quadrangle, was used to characterize the pre-inlet stabilization bathymetry.

---

<sup>1</sup>Taylor Engineering, Inc., 9086 Cypress Green Drive, Jacksonville, FL 32256, U.S.A.



**Figure 1** Location Map of the St. Augustine Inlet Vicinity

A 1974 survey of the Atlantic Ocean waters in the St. Augustine Inlet vicinity conducted by the National Ocean Survey (NOS) served as the primary bathymetric survey for this year. Another 1974 survey, performed by the COE, provided bathymetric information for the inlet throat and adjacent Atlantic Ocean waters. These surveys were supplemented as follows. Depths of inlet interior waters for 1974 were obtained from a National Oceanic and Atmospheric Administration hydrographic chart. Depths along a small region were obtained from a 1975 Florida Coastal Engineers (1976) survey of the nearshore north and south beaches. Additional subaerial elevations along some locations were obtained by adjusting 1972 and 1984 Florida Department of Environmental Protection (FDEP) survey data to 1974 conditions.

In October 1994, Taylor Engineering surveyed the interior waters of St. Augustine Inlet. The untoward occurrence of winter storms precluded survey of the inlet exterior waters that year. Taylor Engineering subsequently surveyed the inlet throat and nearby offshore waters in July 1995. The FDEP surveyed the subaerial beach system along the north and south beaches in September 1995. The combination of these three surveys served to define the inlet vicinity for 1995.

### Region of Inlet Influence

The region of inlet influence is about 19,000 ft to the north and about 30,000 ft to the south of the inlet based upon shoreline and subaerial beach volume change analyses.

### Bathymetric and Subaerial Beach Analysis

All the surveys were reduced to a common digitized format by representing the bottom elevations with respect to mean low water (MLW) at known horizontal locations. These discrete, digitized data were input to digital terrain modeling software. Using triangulation techniques, the software created continuous, three-dimensional surfaces of the inlet bathymetry for 1937, 1974, and 1995. Overlaid, these surfaces lent themselves to accurate computations of bathymetric change.

The 1937—1974 bathymetric comparison was used to estimate the beach and inlet short-term response to inlet relocation and structural improvements (Srinivas et al., 1996). The 1937 surface was also used to generate the bathymetric grid for the pre-inlet stabilization hydrodynamic model, described later. The 1974—1995 bathymetric comparison was used to estimate the present, long-term inlet impacts on the inlet-beach system. For this purpose, erosion-deposition volumes were computed in different submerged regions of the inlet vicinity, as presented in Table 1.

Though the north beach was erosive along almost its entire longshore length, this erosion was generally confined to the nearshore region close to the shoreline. The average total vertical change at any eroding location was generally of the order of 3 ft or less. The inner and outer ebb shoal areas experienced significant changes. Intensive accumulation of sand occurred in the outer ebb shoal region as the ebb shoal expanded eastward. Another notable feature, consistent with measured south beach shoreline

**Table 1** Subaqueous Volume Change Rates ( $10^3$  cy/yr)<sup>1</sup>

Interval	North Beach	Ebb Shoal	Inlet						South Beach
			Throat	Interior	North Channel	South Channel	Inner Salt Run	Outer Salt Run	
1974—1995	-198.4	405.7	-26.7	76.6	5.8	-14.5	94.6	42.6	-340

<sup>1</sup> - denotes erosion, + denotes accretion

advancement adjacent to the south jetty, was the accretion of the beaches immediately south of the inlet as the ebb shoal welded to the shore. The inlet throat experienced substantial changes as the natural channel migrated south. The north channel experienced net accretion whereas the south channel experienced net erosion. Salt Run was almost entirely accretionary. The south beach experienced considerable net erosion. Generally, most of the erosion occurred close to shore and the magnitude of erosion exhibited a slow decrease from north to south.

Also, between 1974—1995, the subaerial beach typically eroded modestly on the north beach while eroding chronically on the south beach; however, the subaerial beach accreted immediately north and south of the inlet due to ebb shoal sheltering effects.

### Ebb Shoal Evolution

During the inlet stabilization period, the system of shoals close to the old inlet channel started to collapse, consolidate, and emerge. Finally, by 1957 and into the post-stabilization period, the shoals welded to the mainland to form a continuous beach south of the inlet.

The ebb shoal was defined according to the method outlined by Dean and Walton (1973). Calculated from this procedure, the ebb shoal volume was about 29 million cubic yards (cy) in 1937 (Table 2). After 1940, the ebb shoal migrated in both the northerly and westerly directions in response to inlet relocation. By 1974, the relocated ebb shoal had about 14 million cy of sand. With continued growth, the ebb shoal had accumulated about 23 million cy of sand by 1995.

**Table 2** Ebb Shoal Volumes

Year	Volume ( $\times 10^6$ cy)
1937	29
1974	14
1995	23

These ebb shoal volumes contrast sharply with the values reported about two decades ago. Upon investigating 44 inlets including St. Augustine Inlet, Walton and Adams (1976) developed a useful relationship between inlet tidal prisms and equilibrium

ebb shoal volumes. They estimated the 1957 ebb shoal volume for St. Augustine Inlet as 106 million cy. Given the northerly ebb shoal migration in response to inlet relocation in 1940 and the south jetty construction in 1957, together with the continuous accretion of the post-inlet stabilization ebb shoal, the 1957 ebb shoal volume is expected to be less than the 1974 ebb shoal volume. However, Walton and Adams' estimate for the 1957 ebb shoal volume is almost an order of magnitude greater than the 1974 ebb shoal volume estimate of the present study. Though the source of Walton and Adams' bathymetric data is not documented, NOS hydrographic and navigation charts (scales 1:10,000—1:40,000) were typically used in estimating ebb shoal volumes. The limited resolution of data obtained from such charts might contribute to some differences in estimates; however, the magnitude of the discrepancy is hard to explain. Walton and Adams also failed to document the planform area used in the volume computations. Given the relative higher resolution of the bathymetric data used in the present study, the current estimates are believed to be more reliable.

Finally, it is interesting to compare the present estimate of the St. Augustine Inlet ebb shoal volume with the equilibrium volume predicted by the functional relationship developed by Walton and Adams (1976) which relates equilibrium ebb shoal volumes, tidal prisms, and degree of beach exposure. In particular, they predict the relation

$$V_{shoal} = 10.5 \times 10^{-5} P^{1.23} \quad (1)$$

for the vicinity of St. Augustine where  $V_{shoal}$  is the equilibrium ebb shoal volume in cubic yards while  $P$  is the tidal prism in cubic feet. According to their estimates, the tidal prism was  $13.1 \times 10^8 \text{ ft}^3$  in 1957; whence Equation 1 predicts an equilibrium ebb shoal volume of 17.2 million cy. Notably, this ebb shoal volume is of the same order of magnitude as the current estimate and substantially less than the Walton and Adams estimate. As computed later, the ebb tidal prism for current conditions is estimated to be about  $13.6 \times 10^8 \text{ ft}^3$ . Applying Equation (1) yields a predicted equilibrium ebb shoal volume of 18 million cy. In contrast, the current ebb shoal volume is about 23 million cy and growing steadily with no evidence of abatement. In conclusion, the exact applicability of the Equation (1) relationship between equilibrium ebb shoal volumes and the tidal prism for St. Augustine Inlet is questionable.

### Littoral Drift

The revised Wave Information Study (WIS) hindcast (Hubertz et al., 1993), believed to be the most reliable long-term wave climate information available, was chosen for estimating littoral drift in the area of interest. Twenty years of hindcast hourly wave data and the orientation of the local shoreline in the region of inlet influence were utilized to evaluate characteristic annual variations in longshore transport with the CERC (COE, 1984) littoral drift formula. Table 3 presents the results of the analysis for the region just north of the region of inlet influence. The average net drift is about 212,000 cy/yr from the north to the south. The magnitudes of the standard deviations indicate a fairly uniform yearly gross longshore transport rate; however, the northward, southward, and especially the net transport rates vary considerably from year to year. The analysis

**Table 3 Littoral Drift for the North Beach Just Outside the Region of Inlet Influence**

Longshore Transport Component	Average Magnitude cy/yr	Standard Deviation cy/yr
Northward	264,000	71,000
Southward	475,000	141,000
Net	212,000	175,000
Gross	739,000	139,000

revealed that the net transport rate is negligibly small for some years, and is actually reversed (south to north), albeit of small magnitude, for some other years.

### Mechanical Bypassing

Over the period of interest (1974—1995) for sediment budget computations, about 480,600 cy of sand (a rate of 21,800 cy/yr) were dredged from locations east of the inlet entrance and placed in nearshore waters off the south beach (St. Augustine Beach).

### Sediment Budget

A sediment budget is a comprehensive delineation of sediment transport pathways and magnitudes (Figure 2). Such a delineation, possible from results of the preceding analyses, is necessary to establish the sources and magnitude of sand being trapped by the ebb shoal and the inlet interior and to quantify sand loss rates from the south beach area.

About 212,000 cy/yr (the littoral drift) of sand enter the north beach from the north due to wave-driven littoral drift. About 5,500 cy/yr erode from the subaerial regions and about 198,400 cy/yr erode from the subaqueous regions of the north beach. Thus, about 415,900 cy/yr of sand move into the ebb shoal area from the north.

The ebb shoal vicinity gains sand at a substantial rate—about 405,700 cy/yr (after mechanical bypassing). The subaerial beach fronting the ebb shoal immediately north of the inlet accretes at a rate of 3,785 cy/yr whereas the subaerial beach fronting the ebb shoal immediately south of the inlet accretes at a rate of 14,900 cy/yr. Further, the inlet throat and the south channel erode at rates of 26,700 and 14,500 cy/yr while Outer Salt Run, the inlet interior, and the north channel accrete at rates of about 42,600, 76,600, and 5,800 cy/yr, respectively. Thus, about 83,800 cy/yr of sand deposit inside the inlet as flood shoals. About 21,800 cy/yr of sand is mechanically bypassed from the ebb shoal vicinity to the south beach vicinity. Balancing the influx of sand into the ebb shoal area from the north, losses to the inlet, efflux due to dredging, and accumulation shows that about 114,100 cy/yr of sand move into the ebb shoal area from the south beach vicinity.

The subaerial regions of the south beach erode about 59,400 cy/yr while the subaqueous regions of the south beach erode about 340,000 cy/yr. Thus, about 307,100 cy/yr move south out of the southern limits of the area of inlet influence. This value is

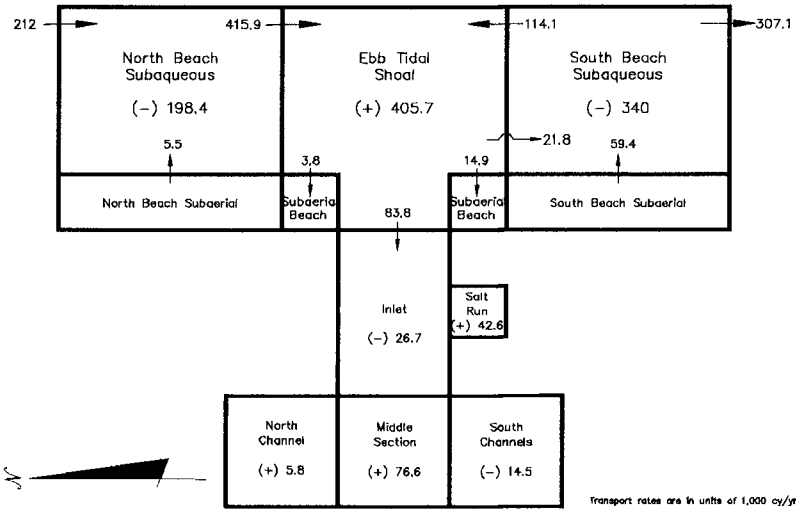


**Figure 2** Sediment Budget (1974-1995) for the St. Augustine Inlet Vicinity

within 7% of the 330,000 cy/yr potential longshore transport rate computed by the independent analysis of spatial distributions of littoral drift. The potential longshore transport rate estimates should be reasonably accurate away from the region of inlet influence due to the diminished impacts of inlet hydraulics. Thus, given the preceding sediment balance, the supply of sand for beaches about 30,000 ft south of the inlet is sufficient to balance the sand requirement demanded by the local nearshore wave climate; this facet is consistent with observed beach behavior.

In summary, the ebb shoal draws sand from both the north and south beaches. Acting as a sink, the ebb shoal area accumulates sand at the rate of 427,500 cy/yr (after discounting the mechanical bypassing volume). The flood shoals gain sand at the rate of about 83,800 cy/yr. Consequently, sand does not naturally bypass the ebb shoal. The 330,000 cy/yr sand requirement of the region south of the zone of inlet influence, as predicted by the potential longshore transport capacity of waves, is approximately satisfied by sand supplied through aggravated erosion of the south beach.

### Effects of Inlet Hydrodynamics

The constant recurrence of inlet-related tidal currents plays a key role in transporting sediments in the inlet vicinity. Waves transport sand into the inlet vicinity, primarily through longshore transport mechanisms. These sediments get entrained in the tidal currents which flow into the inlet during flood tide and out of the inlet during ebb tide and eventually get deposited as flood and ebb shoals. Thus, an understanding of inlet hydraulics is indispensable to understand the cause-effect relationships governing sediment interactions and exchanges in the St. Augustine Inlet vicinity. This was accomplished by the setup and application of numerical models of the St. Augustine Inlet vicinity for the post-stabilization (1994) and pre-stabilization (1937) conditions. Pre-stabilization model results are only briefly described in this paper, complete results for all conditions are presented in Srinivas et al. (1996). The modeling was used to define spatial and temporal distributions of currents in the vicinity of St. Augustine Inlet to develop an understanding of the hydraulic characteristics for the two stages of the inlet's existence. Further, using existing conditions as a baseline for comparison purposes, the inlet model is necessary to assess the unique impacts of proposed inlet modifications on these conditions to evaluate their relative merits (Srinivas et al., 1997).

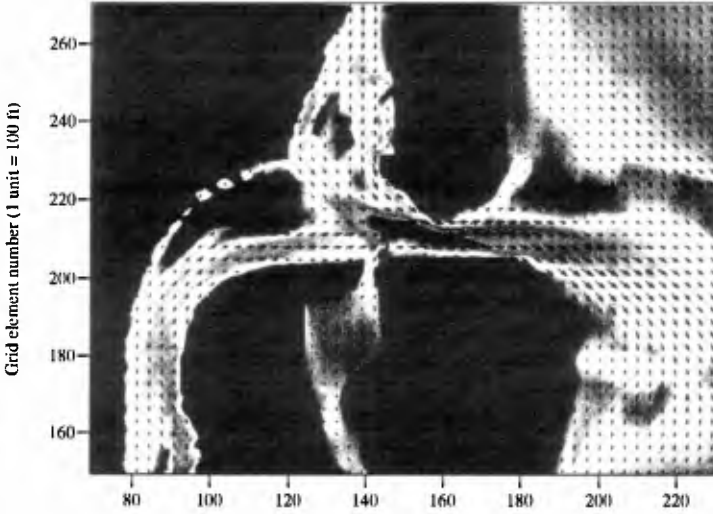
The inlet model is the hydrodynamics portion of TRANQUAL, originally developed by Taylor and Dean (1972) and updated and refined by Taylor and Pagenkopf (1981). TRANQUAL, a vertically integrated, two-dimensional model, uses an implicit finite difference numerical scheme to solve the governing equations of fluid motion and conservation of mass. The formulation incorporates a full treatment of the nonlinear propagation of long waves in complex, shallow estuaries. The model domain extends 334,000 ft and 287,000 ft, centered about the inlet, in the approximate north-south and east-west directions, respectively. The grid scheme consists of 95,858 grid elements, each of dimensions 100 × 100 ft, arranged in a 287 × 334 matrix.

To provide model boundary conditions, Taylor Engineering collected synoptic tide data using bottom-mounted pressure sensing tide gages offshore and inshore the inlet. This data was used to provide the offshore tide forcing and for model calibration.

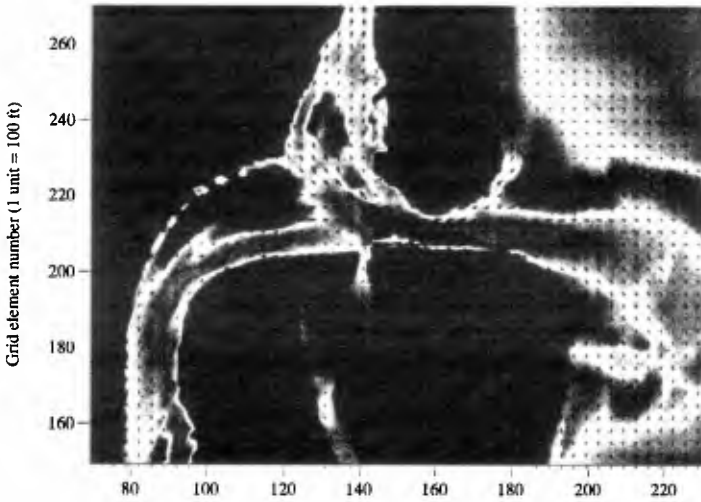
Figure 3 presents a snapshot of the ebb velocity vectors in the inlet vicinity at approximately the time of peak flow velocity through the inlet throat. The vectors are overlaid on an image of the inlet bathymetry. Most of the flow in the inlet interior occurs along the east banks of the Tolomato and Matanzas Rivers. The maximum velocities are generally about 1 ft/sec. The flow accelerates on approaching the inlet throat and velocities of about 2 ft/sec occur immediately west of the inlet throat. Flow velocities in Salt Run are minimal. The flows from the Tolomato River, the Matanzas River, and Salt Run converge just west of the inlet throat and accelerate to velocities of about 3.8 ft/s just north of the south jetty towards the western region of the throat. Thus, flow through the inlet concentrates towards the southern regions of the throat where greatest depths occur. Regions towards the north of the throat are almost stagnant with flow velocities less than 1 ft/sec. Though velocities of around 3 ft/sec occur in some regions of the throat further east, the bulk of the flow exits the inlet at about 2 ft/sec. The 2-ft/sec contour persists into the channel through the ebb shoal until about 3,000 ft east of the inlet entrance. Upon exiting the inlet, the flow immediately curves southeast. Velocities elsewhere in the ocean are of the order of 1 ft/sec or less. Interaction of the ebb flow with the north jetty is minimal. A north to south circulation exists further offshore. Thus, the majority of the conveyance through the inlet throat is through the deep water channel in the south.

Figure 4 presents a snapshot of the flood velocity vectors in the inlet vicinity at approximately the time of peak flow velocity through the inlet throat. The vectors are of the same scale as in Figure 3. The south to north circulation in the offshore is consistent with the higher water level to the south during flood flow. Velocities in the ocean are of the order of 1 ft/sec or less. Immediately east of the throat, flood flow patterns are more symmetrical compared to the ebb flow patterns in the same region. Upon entering the throat, the flow accelerates to about 3 ft/sec as it feels the effects of the north jetty. The shoal regions in the north of the throat, which were relatively stagnant during ebb, now experience velocities of the order of 1 to 2 ft/sec. Thus, the flow becomes relatively well distributed in the eastern regions of the throat. However, the flow skews towards the south (in the deep water channel) in the western regions of the throat. Velocities of the order of 2 to 3 ft/sec, with peaks of about 5 ft/sec, occur in these southern regions. The bulk of the flow decelerates and exits the throat at velocities of about 1 ft/sec; however, higher flow velocities, of the order of 2 to 3 ft/sec, occur immediately northwest of the throat. Upon exiting the throat, most flow is diverted into the Tolomato River with lesser flow entering the Matanzas River. Flow velocities are between 1 to 2 ft/sec in the Tolomato River while the velocities are generally 1 ft/sec or less in the Matanzas River. Flow velocities are less than 1 ft/sec in Salt Run. In summary, the flow is relatively better distributed in the inlet vicinity during flood as compared to the ebb conditions. Peak flood velocities are also higher than the peak ebb velocities.

Discharge time histories through various cross sections revealed that the peak ebb and flood discharges are very similar everywhere. However, the ebb phase lingers longer



Grid element number (1 unit = 100 ft)  
**Figure 3 Ebb Velocity Vectors**



Grid element number (1 unit = 100 ft)  
**Figure 4 Flood Velocity Vectors**

than the flood phase. Discharge magnitudes through the Matanzas and Tolomato Rivers are of comparable magnitudes; however, flow through Salt Run is very small.

Similar analyses were also conducted for the pre-inlet stabilization condition (Srinivas et al., 1996). Table 4 presents the comparison of the discharge prisms. For the 1994 conditions, as inferred earlier from the discharge time-histories, the ebb prism through the inlet entrance is substantially more than the flood prism. This mismatch was smaller in 1937. Though the ebb and flood prisms through the Tolomato River are better balanced for both the 1994 and the 1937 conditions, the ebb prism is slightly larger than the flood prism for both conditions. Further, the ebb and flood prisms for the 1994 conditions are slightly larger than the corresponding prisms for the 1937 conditions. The ebb and flood flow prisms in the Matanzas River are smaller than the corresponding prisms in the Tolomato River. The ebb prism is substantially larger than the flood prism for the 1994 conditions. For the 1937 conditions, the prism mismatch is smaller. Finally, the ebb and flood prisms through Salt Run are minimal for the 1994 inlet.

**Table 4** Comparison of Ebb and Flood Prisms for 1994 and 1937 Inlets

Location	1994 conditions ( $\times 10^8 \text{ ft}^3$ )		1937 conditions ( $\times 10^8 \text{ ft}^3$ )	
	Flood prism	Ebb prism	Flood prism	Ebb prism
Inlet Entrance	8.75	13.62	7.66	10.00
Tolomato River	4.47	4.83	4.14	4.60
Matanzas River	2.86	4.58	2.71	3.76
Salt Run	0.29	0.70	n/a	n/a
Total Interior	7.62	10.11	6.85	8.36

The final analysis considered the residual (velocity) circulation over a full tidal cycle for the present (1994) and pre-stabilization (1937) inlets. Ebb flow dominance was evident almost everywhere for the 1994 inlet except by the eastern side of the inlet throat and by the shoal to the west of the inlet throat. In fact, the circulation patterns show the convergence of residual ebb and flood flows towards the deep gorge in the inlet throat. Residual ebb flows through the Tolomato and Matanzas Rivers are fairly large. The bulk of the residual flow exits the inlet in a southeasterly direction through the channel across the ebb tidal shoal. Similarly, ebb flow dominance is evident almost everywhere for the 1937 inlet. Residual flows through the Tolomato and Matanzas Rivers are fairly weak. The bulk of the flow moves in a southeasterly direction through the deepwater channel in the inlet. On exiting the inlet, the flow splits and moves both northeast and southeast. In summary, the patterns of residual circulation reinforce the concept of an ebb-dominant inlet for both the present (1994) and the pre-stabilization (1937) configurations.

The flow patterns, discharge prisms, and residual circulation patterns verify an ebb-dominated inlet. Many earlier studies (e.g., Dean and Walton, 1975; Walton and Adams, 1976) indicate that the imbalance between the flood and ebb prisms generally

dictates the locations and volumes of the primary shoals. Large ebb shoals generally form when the ebb prism is large and when the imbalance between the ebb and flood prisms is also large. As shown above, such conditions currently exist at St. Augustine Inlet. The results also suggest that improvements to the inlet should focus on reducing the ebb prism magnitude, concomitant with a reduction of the existing ebb-flood prism imbalance and a more southerly ebb jet redirection. Such inlet hydraulic behavior has the potential to reduce ebb shoal sand trapping, reduce the offshore penetration of the ebb jet (discussed next), move the ebb shoal closer to shore, and improve natural sand bypassing.

### Effects of Inlet Ebb Jet

Strong ebb flows through the inlet set up a relatively large-scale circulation in the ocean which can result in sediment transport towards the inlet. The ebb flow on the seaward side of tidal inlets often occurs as unsteady turbulent flow with many properties similar to jet flow. The jet entrains lateral waters as it spreads and results in the transport of sand towards the inlet. The entrained sediments, together with portions of the wave-driven longshore transport in the vicinity, are often jetted and deposited offshore.

A simple numerical model of the ebb jet, based on the work by Özsoy and Ünlüata (1982), was used to characterize existing jet effects on ebb shoal location and growth since bathymetric analyses for the St. Augustine Inlet vicinity indicated that the ebb shoal is currently growing seaward. For model application, the velocity at the inlet mouth was assumed 3 ft/sec based on characteristic maximum ebb velocities inferred from the inlet hydrodynamic model. The input cross shore bathymetry was the average of shore-parallel depths over a distance spanning 1,200 ft either side of the centerline.

Figure 5 presents the velocity contours in the inlet offshore vicinity superimposed on an image of the inlet bathymetry. An implicit assumption of the present model is that the centerline path is straight and perpendicular to the general shoreline orientation, that is, the southeasterly offshore curvature of the natural channel is not accounted for. Ebb flow decelerates with minimal lateral spreading on exit from the inlet. The jet is fairly compact till it decelerates to 1.5 ft/sec, lateral spreading is accentuated beyond this velocity contour. Velocities of 0.5 ft/sec extend till the outer limits of the model grid—about 10,000 ft from the inlet mouth. Given the general bathymetric and sediment size characteristics offshore the inlet, a critical depth-averaged velocity of 1 ft/sec is necessary to initiate sediment motion. Thus, ebb velocities are sufficiently high to keep sediment in motion to a point about 5,000 ft offshore the inlet. This implies that depositional characteristics should dominate further offshore. Given the limitations of the present analysis, this facet is remarkably consistent with the patterns of recent long-term bathymetric changes where the ebb shoal area was seen to be accreting prominently starting about 5,000 ft offshore from the inlet.

### Conclusions

St. Augustine Inlet is a very efficient sand sink which stores sand stored in ebb and flood shoals. The ebb shoal, estimated to contain about 23 million cy of sand by

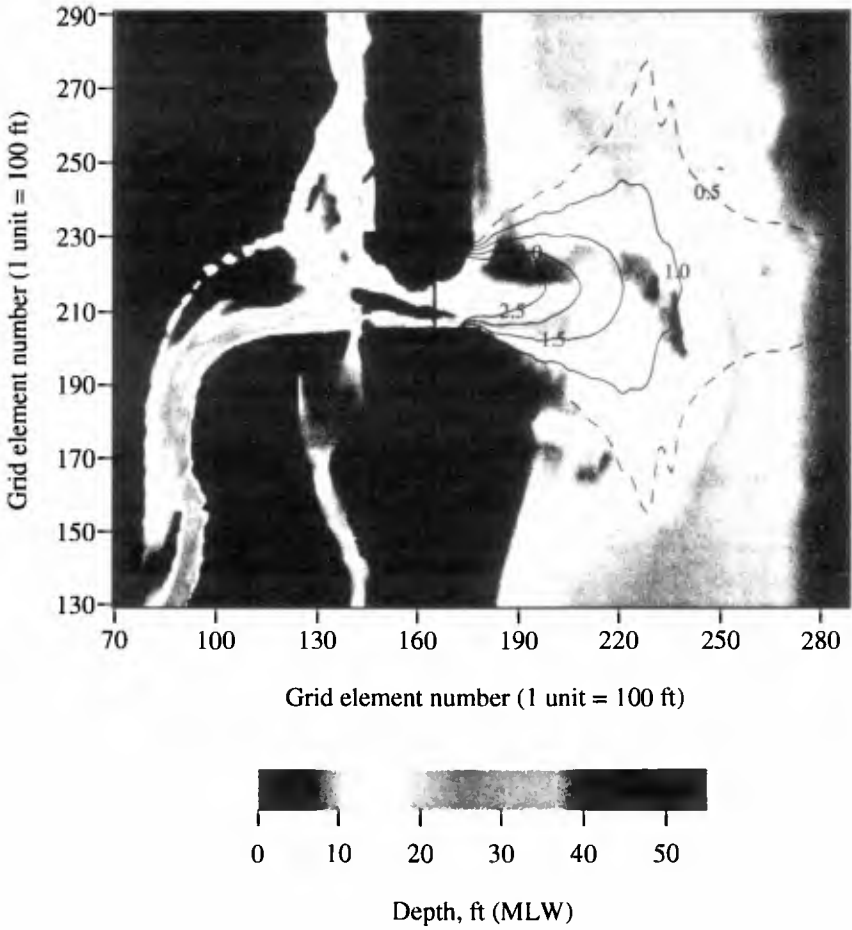


**Figure 5** Ebb Jet Velocity Contours

1994, traps sand at the rate of about 425,000 cy/yr. Flood shoals trap sand at the rate of 84,000 cy/yr. This impoundment of sand deprives the south beaches of sand and causes chronic downdrift erosion. The sand trapping action of the inlet is attributable to the large magnitudes of and the large mismatch between the flood and ebb tidal prisms. The large offshore penetration of the ebb jet is responsible for the ongoing offshore growth of the ebb shoal. Substantial changes to the inlet jetties are possibly necessary to improve the natural bypassing characteristics of the inlet.

#### Appendix A References

- Dean, R. G. and Walton, T. L. 1973. Sediment Transport Processes in the Vicinity of Inlets with Special Reference to Sand Trapping. *Proceedings, 2<sup>nd</sup> International Estuarine Research Conference*, 129—149.
- Florida Coastal Engineers. 1976. *St. Johns County Beach Erosion Study*. Jacksonville, FL.
- Hubertz, J. M., Brooks, R. M., Brandon, W. A., and Tracy, B. A. 1993. *Hindcast Wave Information for the U.S. Atlantic Coast*. U.S. Army Corps of Engineers, Waterways Experiment Station, Vicksburg, MS.
- Srinivas, R., Schropp, S.J., and Taylor, R.B. 1996. *Inlet Baseline Conditions: Physical and Environmental Characteristics, St. Augustine Inlet Management Plan, Part 2*. Taylor Engineering, Inc., Jacksonville, FL.
- Srinivas, R., Schropp, S.J., Trudnak, M.E., and Taylor, R.B. 1997. *Management Alternatives and Recommended Plan Elements, St. Augustine Inlet Management Plan, Part 3*. Taylor Engineering, Inc., Jacksonville, FL.
- Taylor, R. B. and Dean, R. G. 1972. *Numerical Modeling of Hydromechanics of Biscayne Bay/Card Sound System Part II: Dispersive Characteristics*. University of Florida, Department of Coastal and Oceanographic Engineering, Gainesville, FL.
- Taylor, R. B. and Pagenkopf, J. R. 1981. TRANQUAL: Two-Dimensional Modeling of Transport Water Quality Processes. *Proceedings, Stormwater and Water Quality Management Modeling Group Meeting*, U.S. Environmental Protection Agency, Niagara Falls, Canada.
- U.S. Army Corps of Engineers. 1984. *Shore Protection Manual*. Waterways Experiment Station, Vicksburg, MS.
- Walton, T. L. and Adams, W. D. 1976. Capacity of Inlet Outer Bars to Store Sand. *Proceedings, 15<sup>th</sup> Coastal Engineering Conference*, 1919—1937.

#### Appendix B Unit Conversions

English	SI
1 ft	0.3048 m
1 cy	0.7646 m <sup>3</sup>
1 mi	1.6093 km